Development and On-site Construction of GRID NET™ -Grid-type Sabo Dam for Debris Flows of Small Boulders-

Akihiko TAKANO*1, Hiroshi MORIYAMA*1, Takanori KAWAMURA*1, Takuya SAEKI*1, Keita KAGOHASHI*1

*1 Steel Structures & Sabo Division, Engineering Business

The deployment percentage of sabo dams is insufficient for ensuring the safety and protection of human lives against sediment disasters. Therefore, there is a great need for open-type steel sabo dams that have more than twice the sediment-trapping capacity of closed-type sabo dams. However, due to problems with their debris flow trapping capability and with their construction, open-type steel dams have not been used to counter debris flows comprising mostly of small boulders. To address this problem, we have developed GRID NET™, a Kobe Steel-manufactured grid-type sabo dam with a mesh of rings attached to the upstream side that is capable of trapping such debris flows, and so far we have constructed four sabo GRID NET dams. This paper describes the development and construction of GRID NET.

Introduction

The grid-type sabo dam manufactured by Kobe Steel is one kind of open-type steel sabo dam that is constructed from factory-prefabricated steel pipe members with diameters of 508 mm and 609.6 mm and assembled in a three-dimensional grid. By allowing sediment to pass through during low and medium flows to preserve trapping capacity for debris flows, the open-type steel dam is designed to trap large boulders that characteristically accumulate at the front of a debris flow, thereby ensuring a debris flow trapping capacity two to three times greater than a traditional concrete gravity dam.

This capability translates into fewer open-type steel dams being needed to handle debris flows than concrete gravity dams.

At present, the number of sabo dams is still insufficient since approximately only 20% of the needed anti-debris flow dams have been deployed, underlining the need for prompt installation of sabo dams to protect human lives from sediment disasters. However, due to the high construction costs and long construction times needed for sabo dams, at present dam installation progress has fallen behind.

Since the adoption of high-capacity open-type steel dams for trapping debris flows can rapidly achieve an improved deployment percentage and ensure safe and secure living in light of the aforementioned situation, the demand for open-type steel dams has grown substantially. However, despite the substantial demand for such dams at sites of debris flows comprising mostly of small boulders (grain diameter sizes of 500 mm or less), they have not been used because of problems with debris flow trapping and construction.

To resolve the above problems, we have developed GRID NET™ note), a grid-type dam for debris flows of small boulders, which is a traditional grid-type dam with a fine and high-strength mesh of rings attached on the upstream side for trapping such debris[1)]. We have successfully received orders for and completed the construction of four GRID NETs since its development. This paper describes the basic structure of GRID NET, experiments on the efficacy of the mesh of rings for trapping debris flows, drop experiments for boulder impact testing[3)], and on-site construction.

1. Basic structure of GRID NET

Fig. 1 depicts the basic structure of GRID NET. In the basic structure, the net spacing between the vertical steel pipe members of the portion furthest upstream is fixed at approximately 600 mm, to which a mesh of 300 mm diameter rings[4)] is attached. The mesh of rings is a weave of multiple 300 mm diameter rings ("small-diameter rings"), with each ring having multiple circular windings fabricated from a 3 mm diameter steel wire and held together by clips. The mesh of rings is then secured by

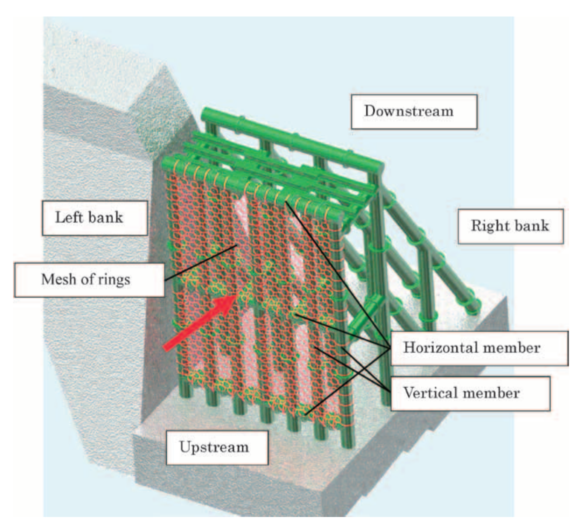

Fig. 1 Basic structure of GRID NET

note) GRID NET is a registered trademark (Nos. 5679434 and 5428784) of Kobe Steel.

shackling the small-diameter rings of the mesh to 550 mm diameter rings ("large-diameter rings") that are mounted to the vertical and horizontal members of the grid-type dam. The advantages of the basic structure are described below.

(1) The standard[2] calls for arranging the vertical and horizontal members at the most upstream part of an open-type steel dam as a planar mesh and further calls for net spacing between each of the vertical members and each of the horizontal members to be no more than the maximum grain diameter, d_{95}[1] (d_{95} is the 95th percentile grain diameter size on the cumulative particle size distribution compiled from over 200 grain samples from the site). If the grid members are arranged as above, the projected area A_0 of the opening framed by the vertical and horizontal members will become smaller than the projected area A_b of the grid members themselves when d_{95} is less than 500 mm. If, as in this case, the void ratio [$n_0 = A_0 / (A_0 + A_b)$] is 0.5 or less, the stream will become dammed[5] on the upstream side of the dam before the debris flow front reaches the barrier, causing the clump of boulders at the debris flow front to disintegrate and the boulders to arrive separately to the barrier. The debris flow is not effectively trapped.
However, since the thin wires of the mesh of rings can achieve a void ratio of 0.5 or greater, the stream does not become dammed and the debris flow can be reliably trapped.

(2) Next, the planar grid-type arrangement for the members furthest upstream was abandoned and replaced with an arrangement of only the vertical members with a net spacing of approximately 600 mm. The decision to do so was based on the rationale that a void ratio of 0.5 or greater can be achieved while also ensuring that a disaster can be suppressed with a narrow 600 mm spacing of members even if, in a rare case, the net fails due to some unanticipated event and the trapped sediment gets released.

2. Experiment to verify the trapping function of the mesh of rings

2.1 Overview of experiment

Table 1 summarizes the series of experiments that were performed. In cases 1-1 to 3-2 in Table 1 (Net model), the maximum grain diameter d_{95} was multiplied by factors of 3.0, 2.0, and 1.5 to provide a varying ring diameter Dr to investigate the effect of the ratio Dr/d_{95} on the debris flow trapping ratio, and in cases 4-1 to 6-2 (bottom beam model), the maximum grain diameter d_{95} was multiplied by factors of 2.0, 1.5, and 1.0 to provide a varying vertical height for the net spacing of the bottom horizontal beam members bh to investigate the effect of the ratio bh/d_{95} on the trapping ratio. Further, in cases 7-1 and 7-2 (Slit model), the net spacing between vertical members b1 was configured to be 1.5 times that of d_{95} in the test unit, without an installation of the mesh, to compare the trapping effectiveness with that of the mesh of rings.

The experiment was scaled to 1:50 and used a rectangular channel that was 300 mm wide and 10 m long with a gradient of 17 degrees. Sediment was packed into a thickness of 10 mm and a length of 1.3 m at a position 5 m upstream of the test unit and was released with a unit flow rate of 0.75 cm^2/s for the experiment. **Fig. 2** shows the particle size distribution of the fluidized sediment. Fig. 2 plots both the experimental sand (d_{95} = 10.1 mm) and the large boulders ($d_{95\ 5}$ = 15.7 mm). The experimental sand is defined to be of grain size of the 95th cumulative percentile of all the sand used in the experiment, and the large boulders are defined to be the grain size of the 95th cumulative percentile of 100 large boulders selected from the experimental

Table 1 Summary of experiments

Case	Model name	Dr/d_{95}	bh/d_{95}	bl/d_{95}
1−1	Net model	3.0	—	—
1−2				
2−1		2.0	—	—
2−2				
3−1		1.5	—	—
3−2				
4−1	bottom beam model	1.5	2.0	—
4−2				
5−1			1.5	—
5−2				
6−1			1.0	—
6−2				
7−1	Slit model			1.5
7−2				

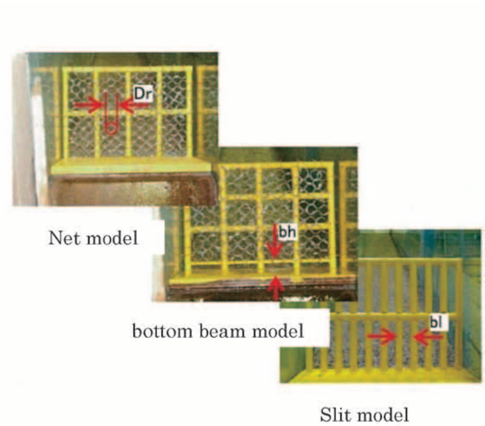

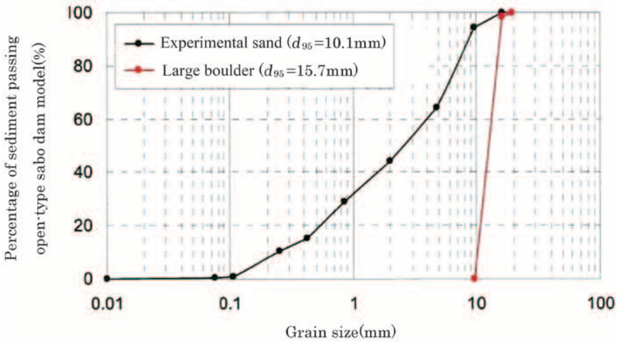

Fig. 2 Grain size distribution of fluidized sediment

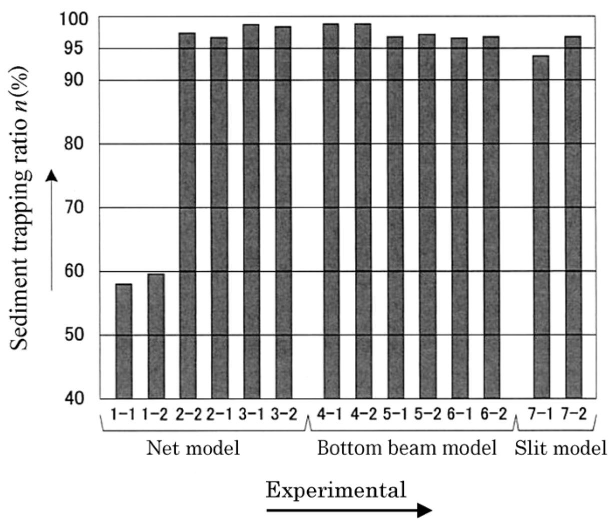

Fig. 3 Experimental results

sand. In this experiment, the latter grain size of 15.7 mm was used as the maximum grain size, or d_{95}.

2.2 Experimental results

The experimental results are shown in **Fig. 3**. The horizontal axis labels in Fig. 3 are the cases of the experiment and the vertical axis is the debris flow trapping ratio n. Here, the trapping ratio n, is calculated as: $n = V1 / (V2 - V3) \times 100$, where $V1$ is the volume of sediment, $V2$ is the volume of all fluidized sediment, and $V3$ is the volume of sediment that overflowed the test unit. Fig. 3 offers the following observations.

(1) Net model

1) The trapping ratio n for cases 1-1 and 1-2 is 60% or less and is lower in comparison with the other cases. This was due to the large value for Dr, which in this case was 3 times the size of d_{95} (Dr/d_{95} = 3.0), which caused the sediment that had initially been trapped to leak through as it was pushed by the flow behind it.
2) For cases 2-2 to 3-2, the ratio n is 95% or greater and the design adequately served its purpose for trapping debris. This means that if Dr is configured to be no more than 2 times the value of d_{95}, the debris flow can be adequately trapped. However, in conformance to the standard[1)] for the actual implementation, we have defined Dr to be no more than 1 times the value of d_{95} in order to trap more reliably. **Fig. 4** shows pictures of the trapped debris flow.

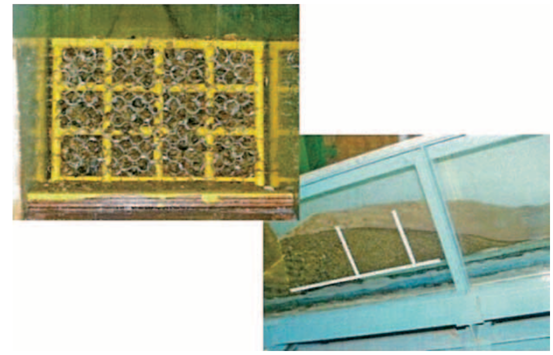

Fig. 4 Trapped debris flow (Case 4-1)

(2) Bottom beam model

1) The trapping ratio n for all the bottom beam model cases was high at 95% or greater. This shows that if bh is no more than two times the value of d_{95}, the debris flow can be adequately trapped.
2) Since the debris flow depth h in the experiment was 40 mm and was larger than bh (10 mm, 15 mm, 20 mm) of the bottom beam model, this means that even if bh is larger than d_{95}, the debris flow can be adequately trapped as long as bh is smaller than h. However, in consideration of safety and the standard[1)] in the case of bh as well, we have defined bh to be no more than the debris flow depth h or to be no more than 1.5 times the value of d_{95}.

(3) Slit model

At the 95% level, the slit model has a high trapping ratio n. A comparison of the slit model n values with the n values for the net model cases 2-2 to 3-2 shows that the net model n has higher values. This means that the trapping efficacy of the mesh of rings is considerably high.

(4) Stream damming

In this series of experiments, the stream never became dammed and we were able to verify that the clump of boulders at the debris flow front reached the model without disintegrating.

3. Experiment to validate the energy-absorbing power of the mesh of rings

Although the mesh of rings is an implementation of a proven wire mesh technique[6)] for trapping debris flows, the method to test the energy absorption, ER, was not known for a mesh of rings covering a narrow rectangular cross-section framed by vertical and horizontal steel pipe members as implemented in this study. Therefore we assumed that *ER* can be expressed as a product of the energy absorbency *En* retained by one ring (as used in rockfall protection works) and the number of rings that covers the rectangular cross section noted above, as shown in Eq. (1). To verify this assumption, we performed full-sized impact tests.

$$ER = En \times nR \quad \cdots\cdots (1)$$

where:

En is the energy absorbency of one ring.
nR is the number of rings.

3.1 Overview of experiment

Table 2 summarizes the series of experiments that were performed and their results. **Fig. 5** illustrates the test unit and test equipment. As shown in Table 2, two stands were used in the experiment. For stand I, the center-to-center spacing of the horizontal members is 1,800 mm and is hypothetically based on the lowest dam height; and stand II is hypothetically based on the highest possible height for a dam and has spacing of 4,150 mm between the horizontal members.

Nr in Table 2 is the number of windings per ring. Cases 1-1 to 4-2 in Table 2 used rings with an *Nr* of 5, with which we investigated the maximum energy absorbency of the mesh of rings. Similarly, cases 5-1 to 6-2 used rings with an *Nr* of 7 and cases 7-1 and 7-2 used rings with an *Nr* of 1. Cases 8-1 and 8-2 used stand II, which has the narrowest rectangular cross section, and rings with an *Nr* of 5.

The test unit was full-sized while GRID NET, as shown in Fig. 5, was partially simulated with a mesh of rings attached to a stand constructed from 508 mm diameter steel pipes. The mesh was installed according to the actual installation method in which the mesh is secured to every other vertical member. Note that *nR* from Eq. (1) is the number of rings

Table 2 Summary of experiments and experimental results

Case	Stand	*Nr* (windings)	*En*(KJ)	*nR* (number of rings)	*ER*(KJ)	*EW*(KJ)	*EW*/*ER*	Results
1−1	I	5	0.34	12.5	4.25	4.25	1.00	Pass
1−2								Pass
2−1						5.31	1.25	Pass
2−2								Pass
3−1						6.38	1.50	Fail
3−2								Pass
4−1						8.50	2.00	Fail
4−2								Fail
5−1		7	0.50		6.25	6.25	1.00	Pass
5−2								Pass
6−1						7.81	1.25	Pass
6−2								Pass
7−1		12	1.10		13.75	13.75	1.00	Pass
7−2								Pass
8−1	II	5	0.34	33.5	11.39	11.39	1.00	Pass
8−2								Pass

Nr(windings) : Number of windings per ring　　*En*(KJ) : Energy absorbency per ring
nR : Number of rings in rectangular section framed by vertical and horizontal members
ER(KJ) : Calculated energy absorbency of mesh of rings
EW(KJ) : Test weight energy
Pass : No mesh failure　Fail : Mesh failure

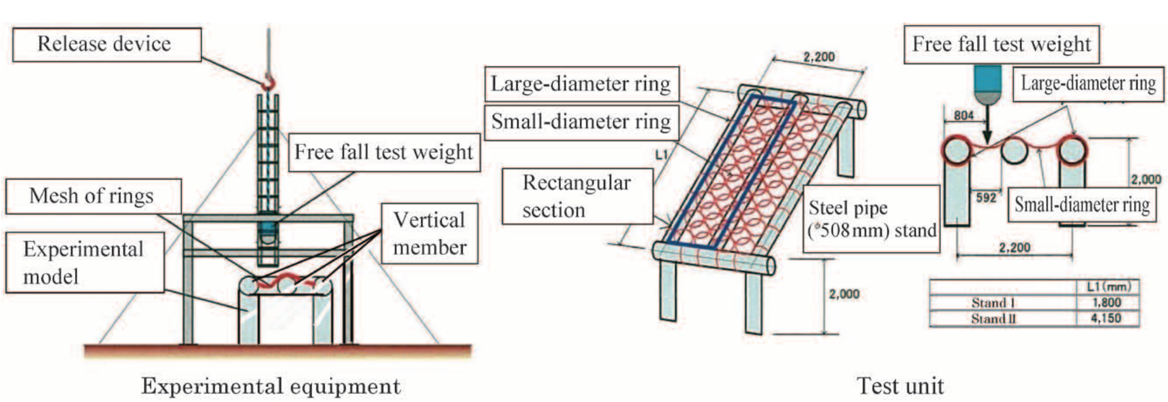

Fig. 5 Experimental equipment and test unit

inside the rectangular cross section indicated in Fig. 5.

As shown in Fig. 5, the experiment was conducted using a test weight to simulate a stone in a free fall drop from a designated height to impact on one side of the mesh.

3.2 Experimental results

The experimental results are as shown in Table 2. **Fig. 6** also shows the condition of the mesh before and after impact by the test weight for case 1-1.

(1) As can be seen from Table 2, the mesh failed in the group of cases from 3-1 to 4-2, but failure was not observed in cases 1-1 to 2-2. *EW* in Table 2 is the potential energy of the test weight that was varied for the testing. The results thus indicate that the mesh of rings with an *Nr* of 5 windings has an energy absorbency that is 1.25 times that of *ER* or more. Further, Fig. 6 shows that the mesh of rings had stretched quite a bit, clearly indicating that energy had been absorbed by its deformation.

(2) We can see from cases 5-1 to 7-2 that a value of 1.0 or greater was achieved for the ratio *EW*/*ER* for the mesh.
These results mean that the mesh possesses the predetermined energy absorbency for *Nr*s of 7 and 12 windings as well.

(3) We can see from cases 8-1 and 8-2 that the mesh achieved a value of 1.0 or greater for the ratio *EW*/*ER*. These results mean that the mesh possesses the predetermined energy absorbency for stand II as well.

(4) Since the energy absorbency *ER* of the mesh of rings was less than *EW* as observed in the discussions (1) through (3) above, we have been able to confirm the appropriateness of using *ER* from Eq. (1) for our designs.

Fig. 6 Condition of mesh of rings

4. Construction of GRID NET

4.1 Preliminary considerations for construction

The actual installation of the mesh of rings to a grid-type dam is performed after the grid-type dam has been constructed and painted, and requires the use of the construction scaffolding and care to avoid damaging the paint during mesh installation. As a study prior to an actual installation, a mock install (or rehearsal) was performed with the conditions stated above. An overview of the study is given below.

(1) The large-diameter rings are multiple windings fabricated from 5 mm diameter wire. We verified that each ring could be easily mounted by unwinding the ends of the wire so as to loosen the strands of the winding and slipping it onto the steel pipe, then turning the rings repeatedly to complete the mounting.

(2) To prevent damage to the paint while the large-diameter rings are mounted, we decided to cover the steel pipes with vinyl tarpaulin. Note that the vinyl tarpaulins are to be removed after installation has been completed.

(3) After the large-diameter rings have been mounted, the ring windings are secured with clips so that the windings do not fray. However, because the clips might have damaged the paint on the steel pipes after the vinyl tarpaulins were removed, the step was taken to cover all the clips with vinyl sleeves.

(4) Scaffolding has traditionally been installed in very close proximity to the vertical members during the construction of a grid-type dam, so there was no space for attaching the mesh of rings. For this reason, the provision was made for a gap of several centimeters, small enough so as not to be a safety issue, between the vertical members and the scaffolding.

(5) **Fig. 7** is a picture of the installation experiment for the mesh of rings. Note that because the mesh of rings is a woven assembly of flexible, 300 mm diameter, small-ringed structures, it has high vertical and horizontal elasticity. For this reason, there was a possibility that an error might occur between the final dimensions of the actual item and the final design dimensions. The concern was that if the error were significant, the attached mesh of rings would sag more than expected or would be too taut, so we also verified the mesh tension during the mock install. As a result, we were able to verify that the mesh of rings did not have unexpected sag or tautness and that it can be installed without problems.

4.2 Construction of GRID NET

GRID NET was selected for installation at: the Shokanbogawa sabo dam site for the Tannan Civil Engineering Office of Fukui Prefecture in fiscal year 2011; the Higashinikkawa sabo dam site for the Hokushin Construction Office of Nagano Prefecture in fiscal year 2012; the Obama sabo dam site for the Junreidani sabo dam site for the Obama Civil Engineering Office of Fukui Prefecture in fiscal year 2013; and the Hinoki-no-Hazakawa sabo dam site for the Central Prefectural Land Development Office of Shimane Prefecture in fiscal year 2014.

Fig. 8 is a diagram of the attachment procedures for the mesh of rings at the Shokanbo sabo dam. Below is a description of the installation based on Fig. 8.

1) After the dam has been constructed, the scaffolding already in place is used to wrap the vertical and horizontal members with vinyl tarpaulin to protect the painted surfaces of the steel pipes.
2) The large-diameter rings are mounted on the vertical and horizontal members.
3) Vinyl sleeves are installed over the clips that secure the large-diameter rings.
4 A crane hooks onto the second row of small-diameter rings on the mesh of rings to raise and suspend the mesh. The top row of small rings is kept free since these need to be shackled to the top row of large-diameter rings.
5) First, the top row of small-diameter rings are manually pulled into their designated positions and shackled to the large-diameter rings. Then the small-diameter rings are shackled to the large-diameter rings on the vertical members and in turn to the large-diameter rings on the bottom row. This work was performed manually and relatively easily.
6) After the mesh of rings has been attached, the quality of the installation is checked, and overall work adjustments are made.
7) Lastly, the vinyl tarpaulins are removed.

We were able to complete the series of tasks in approximately one and a half days without major problems. This was possible because we had thoroughly conducted a preliminary study of the installation. **Fig. 9** is a picture of the mesh of rings

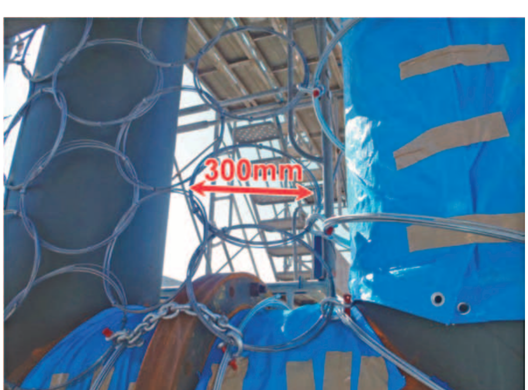

Fig. 7 Attachment of the mesh of rings

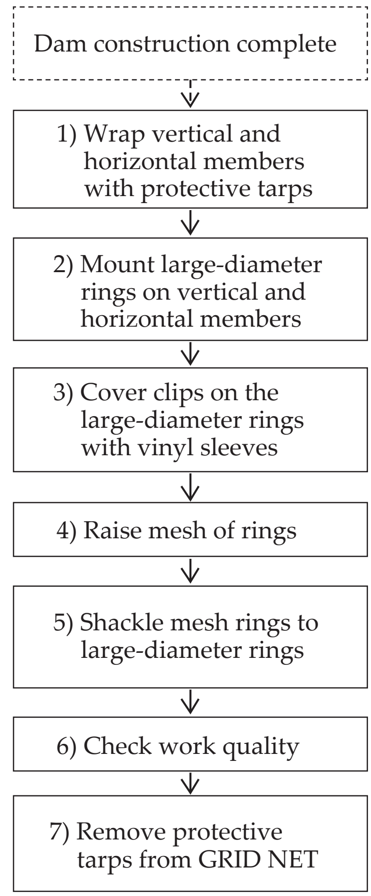

Fig. 8 Installation procedure for the mesh of rings

Fig. 9 A completed GRID NET

after installation. In Fig. 9, we can see that the mesh has been installed without excessive sag.

Conclusions

We have developed and achieved commercial viability with GRID NET (Grid-type Sabo Dam for Debris Flows of Small Boulders), a dam capable of handling debris flows containing small boulders, which have been beyond the application scope of open-type steel dams. We believe the achievement of such an expansion in the application scope of open-type steel dams with extremely large debris flow trapping capacities will have a significant impact on improving the deployment percentage of sabo dams. Furthermore, as a dam for mitigating disasters, GRID NET is also capable of handling fine particle grains when such grains must be prevented from flowing downstream. GRID NET is expected to protect lives and assets from sediment disasters and to enhance the safety and security of residents.

Going forward, we will maintain a sustained effort to perform follow-up investigations of the existing GRID NET installations and to keep verifying their functional efficacies for letting sediment pass through during low and medium flows but to trap debris during large flows, and to keep verifying the durability of the mesh of rings after a debris flow has been trapped.

References

1) H. Moriyama et. al. *Journal of the Japan Society of Erosion Control Engineering*. 2010, Vol.62, No.6, p.30-33.
2) Ministry of Land, Infrastructure, Transport and Tourism. *Manual of Technical Standard for establishing Sabo master plan for debris flow and driftwood*. 2007.
3) T. Kawamura et. al. *Fiscal Year 2010 Proceedings of the Annual Conference of the Japan Society of Erosion Control Engineering*. 2010, p.210-211.
4) TOA Grout Kogyo (Sabo Engineering) *Report*. 2002, (Received 31 July 2009; Accepted 26 January 2010).
5) Y. Hasegawa et. al. *Journal of the Japan Society of Erosion Control Engineering*. 2003, Vol.55, No.6, p.66-73.
6) K. Shimojo et. al. *Journal of the Japan Society of Erosion Control Engineering*. 2010, Vol.62, No.6, p.38-42.